




Article

A Model-Driven Approach for Estimating the Energy Performance of an Electric Vehicle Used as a Taxi in an Intermediate Andean City

Jairo Castillo-Calderón ^{1,2} , Daniel Cordero-Moreno ³  and Emilio Larrodé Pellicer ^{4,*} 

¹ PhD Program in Mechanical Engineering, University of Zaragoza, C. de Pedro Cerbuna, 12, 50009 Zaragoza, Spain; 894645@unizar.es or jdcastilloc@unl.edu.ec

² Scientific Experiences in Mobility, Vehicles and Transport (eX-MoVeT) Research Group, Faculty of Energy, Industries and Non-Renewable Natural Resources, Universidad Nacional de Loja, Av. Pio Jaramillo Alvarado, Loja 110103, Ecuador

³ Faculty of Science and Technology, Universidad del Azuay, Av. 24 de Mayo 7-77, Cuenca 010204, Ecuador; dacorderom@uazuay.edu.ec

⁴ Department of Mechanical Engineering, University of Zaragoza, C. de Pedro Cerbuna, 12, 50009 Zaragoza, Spain

* Correspondence: elarrode@unizar.es

Abstract: Regarding the decision to opt for vehicles with electric propulsion systems to achieve a sustainable future, much research has focused on the electrification of passenger cars, since this class of vehicles is the largest contributor of greenhouse gas emissions in the transportation sector. The purpose of this paper is to assess the energy performance of an electric vehicle used as a taxi in Loja, Ecuador, an intermediate Andean city, using a model-driven approach. Data acquisition was performed through the OBDII port of the KIA SOUL EV for 24 days and the variable mass of the vehicle was recorded as a function of the number of passengers; the effects of road gradient were also considered. The energy performance of the vehicle was simulated by developing an analytical model in MATLAB/Simulink. An average measured battery performance of 8.49 ± 1.4 km/kWh per day was obtained, where the actual energy regenerated was $31.2 \pm 1.5\%$. To validate the proposed model, the results of the daily energy performance estimated with the simulation were compared with those measured in real driving conditions. The results demonstrated a Pearson correlation coefficient of 0.93, indicating a strong positive linear dependence between the variables. In addition, a coefficient of determination of 0.86 and a mean absolute percentage error of 3.35% were obtained, suggesting that the model has a satisfactory predictive capacity for energy performance.

Keywords: electric taxi; energy performance; model-driven approach; real driving conditions



Citation: Castillo-Calderón, J.; Cordero-Moreno, D.; Larrodé Pellicer, E. A Model-Driven Approach for Estimating the Energy Performance of an Electric Vehicle Used as a Taxi in an Intermediate Andean City. *Energies* **2024**, *17*, 6053. <https://doi.org/10.3390/en17236053>

Academic Editor: Hugo Morais

Received: 18 September 2024

Revised: 18 November 2024

Accepted: 25 November 2024

Published: 2 December 2024



Copyright: © 2024 by the authors. Licensee MDPI, Basel, Switzerland. This article is an open access article distributed under the terms and conditions of the Creative Commons Attribution (CC BY) license (<https://creativecommons.org/licenses/by/4.0/>).

1. Introduction

Electric vehicles (EVs) are envisioned as a possible solution to achieve a sustainable future [1–6]. By the end of 2020, more than 10 million EVs were reported globally, following a decade of rapid growth, as seen in Figure 1. Specifically, global EV registrations increased by 41% in 2020, despite the pandemic-related global recession, where global car sales fell by 16%. In total, sales of around 3 million EVs were reported in 2020 [7]. Although different market analysts forecast a high global penetration of EVs, increasing to 33% by 2040 and 50% by 2050, the truth is that they currently represent a small fraction of the transportation sector [8]. In fact, in countries that have introduced EVs, such as China, Germany, the United States, France, Switzerland, and South Korea, the proportion of EV sales in each country is still below 5% of total vehicle sales [9]. Related to this, most electric vehicles are concentrated in a few countries, or regions, with high market shares, such as China, which accounted for more than 50% of electric vehicles globally in 2022, followed by Europe with 30% and the US with 10% [10]. The main risk factors for this low EV uptake are

associated with insufficient range, initial purchase costs, battery costs, and poor charging infrastructure [11,12].

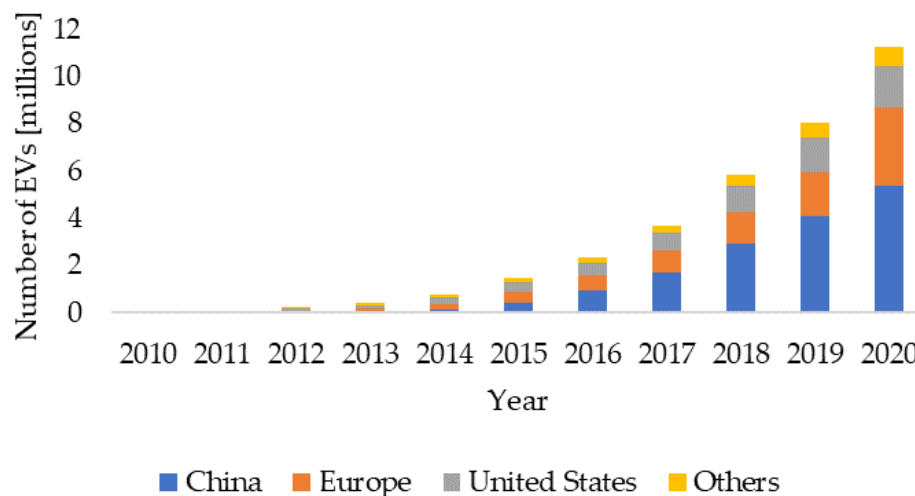


Figure 1. World stock of EVs by region [7].

Ecuador is no stranger to this reality, since EV deployment is considerably low. According to [13], 132,388 new vehicles were sold nationwide in 2023. Of these, 1823 were electric vehicles, equivalent to 1.38% of total sales. In contrast to sales records in previous years, it is noteworthy that Extended Range Electric Vehicles (EREVs) were introduced to the national market in 2023, with 1043 units. Consequently, 780 battery electric vehicles (BEVs) were sold this year. Figure 2 shows the historical evolution of electric vehicle sales in Ecuador. Despite the low introduction of electric vehicles in the country, in 2023 there was sales growth of 316.2% compared to 2022.

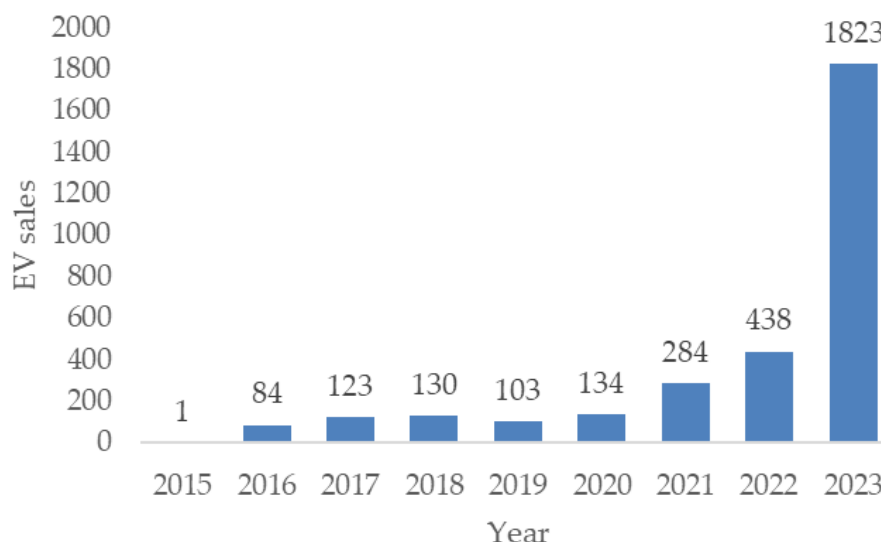


Figure 2. Historical evolution of electric vehicle sales in Ecuador [13].

Figure 3 shows electric vehicle sales in the main provinces of Ecuador for the years 2022 and 2023. A predominance in the introduction of electric vehicles is observed for Pichincha with 61.7%, followed by Guayas with 24.8%. Unlike the aforementioned provinces, the cantonal capitals of Azuay, Manabí, and Tungurahua are considered intermediate cities. It can be seen that there is a lower incursion of electric vehicles in these provinces with smaller populations.

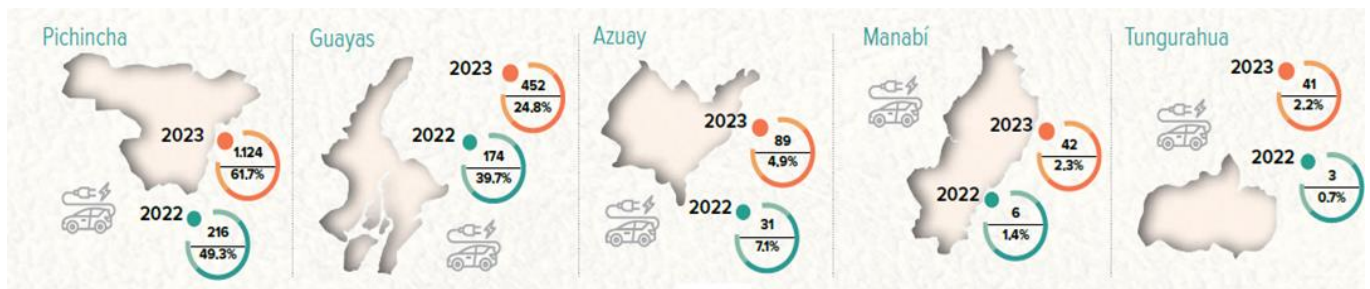


Figure 3. Sales of electric vehicles in main provinces of Ecuador [13].

In 2017, the southern city of Loja pioneered the introduction of 51 EVs into public transportation by integrating them into the existing taxi system [14], forming the company ELECTRIC LOJA ECOLOSUR. In pursuit of this objective, some economic incentives from the government and the local municipality were proposed to current vehicle owners to acquire 16 KIA Soul EV units and 35 BYD e5 EV units. On 26 June 2017, through Municipal Resolution No. 001-CPO-UMTTTSV-2017, the electric cab company obtained the corresponding operating permit [15].

In Ecuador, the transition from fossil fuel-operated vehicles to EVs poses a significant challenge and is imperative from both the energy and environmental perspectives. This necessity arises notably due to the transportation sector’s prominent position as the largest consumer of energy, with a consistent pattern of growth over time, as evidenced by scholarly sources [16,17]. By 2020, Ecuador had an energy consumption of 83,088 kBEP, an increase of 14.3% from 2010, where historically the transportation sector is the one with the highest consumption and has increased its annual share from 41.7% of total energy consumption in 2010 to 45.4% in 2020; this is 30,246 kBEP and 37,744 kBEP, respectively [18], as shown in Figure 4.

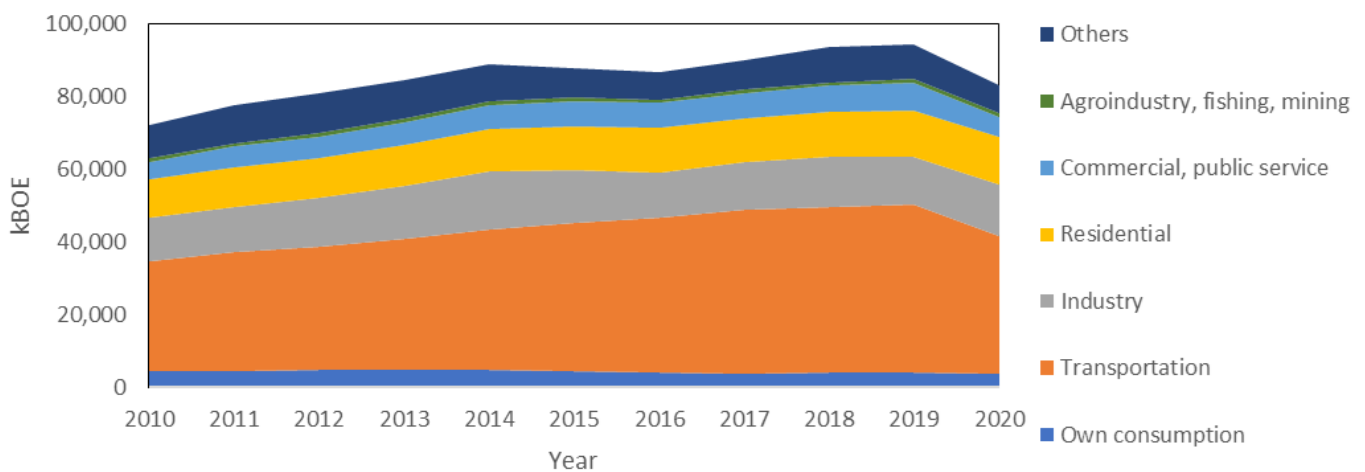


Figure 4. Disaggregation of energy consumption by sector [18].

As a result, the transportation sector is the largest contributor to greenhouse gas (GHG) emissions, accounting for 46.7% in 2020, since 99% of the energy consumed came from diesel and gasoline, as shown in Figure 5.

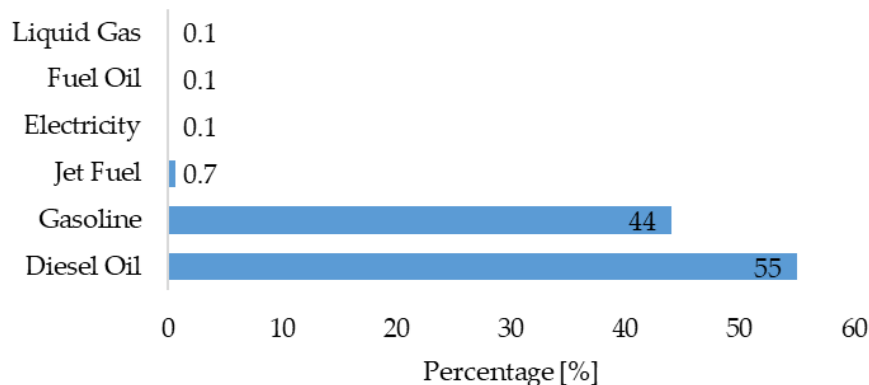


Figure 5. Energy consumption by source in the transportation sector [18].

Some studies have been carried out to promote a more efficient energy transition in Ecuador, and thus to seek the adoption of BEVs. In [19], an evaluation of the state of the Ecuadorian electricity system is presented and through a prospective analysis for the year 2050, hypothetical demand is predicted and a system of electricity generation 100% based on renewable energy sources (hydroelectric, solar photovoltaic, and wind) is guaranteed, positively impacting the economy, increasing production levels, and improving the quality of life of citizens. In the same direction, [20] provides an overview of energy development strategies in Ecuador and proposes energy planning for future years based on technical, economic, and environmental indexes that improve current energy efficiency. Using the EnergyPlan software (version 16.3), exhaustive simulations are carried out to determine the optimal configuration of renewable sources (hydroelectric, solar photovoltaic, and wind, among others) and energy storage required in the future, obtaining an optimal result balanced between the technical-economic factors, the stability of the massive electrical system, and the availability of resources. Ref. [21] presents a long-term roadmap for the comprehensive electrification of mobility for the intermediate city of Cuenca, Ecuador; it seeks to take advantage of the renewable energy potential available in the region. The results indicate that the energy mix would be composed of wind (37.3%), solar photovoltaic energy (33.9%), and hydroelectricity (25.4%). Other technologies such as biomass do not exceed 3.4%. In [22], models are proposed to determine an optimal and sustainable supply for the coming years in the Ecuadorian electricity system. The incursion of renewable sources is proposed to reduce dependence on hydrocarbons, taking as a starting point real data from the current system. In addition, a growing demand for the year 2027 is considered, which includes 100,000 EVs in the analysis. The results show that carbon reduction in the future is feasible and that increasing the capacity of renewable sources up to a certain limit is viable. In [23], a LEAP model is proposed for forecasting Ecuador's energy sector. The model results in a final energy consumption of 158 million BOE in 2030, where the transportation sector is the main energy consumer. Regarding Ecuador's energy planning, a production of 63 513 Gwh is forecast in 2030, derived from hydroelectricity. The results indicate that energy efficiency policies for the transport sector would reduce the use of petroleum derivatives.

Building upon the preceding discussion regarding the choice to adopt vehicles with electric propulsion systems for advancing toward a sustainable future, the majority of research has focused on the electrification of passenger cars, since they are the largest contributors to transport emissions, with 3 GtCO₂ in 2020, equivalent to 41.10% [24]. Therefore, this vehicle class presents an opportunity for massive gains in combating the growing GHG effect [25].

Thus, the objective of this research is to compare the simulated energy performance of an electric cab with that measured under real driving conditions. The research was carried out in Loja, an intermediate Andean city with an urban population of more than 250,000 inhabitants. The city is located at an altitude of 2060 m above sea level, in the southern highlands of Ecuador, and has a particularly mountainous terrain. The study is

all the more important because of the uncertainty and disagreement of cab owners due to poor cab performance, which directly affects their income. The initial performance reported by dealers at the time of sale in terms of vehicle autonomy and energy consumption, according to the New European Driving Cycle (NEDC), is far from the real one [15]. Indeed, it is observed that the autonomy significantly diminishes during the initial year of operation, and there remains uncertainty regarding the actual energy consumption of the units during urban driving conditions. The problem has reached such a point that, on 12 July 2022, the municipal council approved the reform of the ordinance that establishes the creation and regulation of the ecological-electric cab service in the canton of Loja, where members can change from an electric cab to a conventional cab if necessary [26]. In this context, the current study proposes a model-driven approach aimed at estimating the energy consumption of a BEV functioning as a taxi within the urban area of the city. These estimations are subsequently validated through a comparative analysis with actual energy consumption data.

2. Literature Review

A number of studies have been developed around the world aimed at the evaluation of BEV energy consumption. For example, a simulation-based commercial BEV energy consumption approximation approach using real-world driving cycle data in urban areas is proposed in [27]. Although the results are promising, the energy consumption simulation does not consider road slope, which limits the actual operating condition of the vehicle. In [28], the effects of different environmental and control parameters on BEV energy consumption and range are analyzed. For this purpose, they establish a digital twin simulation model in GT-Suite software. The model is calibrated using experimental data based on standardized driving cycles.

An approach to analyzing the impact of traffic on BEV energy consumption is provided in [1]. Thirty different drivers drove a 2017 Volkswagen eGolf twice a day on a predetermined route; in this way, the human element of individual driving behaviors was considered. It is to be emphasized that the methodology did not define the typical driving cycle of the selected route, where its characteristic parameters could be denoted. In [29], the impact of the combination of fast DC charging, higher aerodynamic loads, auxiliary loads, reduced battery capacity, and high-speed driving on the energy consumption and driving range of two BEVs, a Nissan Leaf and a Mitsubishi iMiEV, is discussed. The driving experiments were conducted on a flat section of highway in Perth, Western Australia, at different speeds. It should be noted that the study did not consider the effects of the highway's slope profile and that a typical driving cycle was not defined for the selected route.

In [30], the energy consumption modeling of a BMW i3 is performed using MATLAB/Simulink software. The BEV model demonstrated a level of accuracy with less than 6% error between the simulation and experimental results for the standardized EPA and NEDC cycles. That is, the study does not consider real driving cycles. In [31], the instantaneous energy consumption of BEVs is calculated using the instantaneous power exerted, where the vehicle speed profile and the second-by-second acceleration level are used as input variables. For model validation, the Nissan Leaf EV vehicle was used and various standardized driving cycles were applied. As part of future endeavors, the authors intended to gather empirical data on the energy consumption of BEVs in real-world settings. Following this trajectory, a theoretical analysis of the energy consumption of a Nissan Leaf according to NEDC and WLTC driving cycles is presented in [32]. With a different approach, in [33], the authors estimate the energy consumption of a Mitsubishi i-MiEV on two predetermined urban routes. To do so, they used a neural network that takes as input data driving style variables and route characteristics, obviating deterministic knowledge of the vehicle characteristics or driving cycles.

In [34], the energy consumption of BEVs is measured and estimated. In detail, the EV used was a conversion of a Nissan D21 pickup truck built by the research team, in which a CAN bus data logger and GPS were installed. However, the data set of this research is

limited, as it contains data from a single driver, a vehicle that is not currently commercially produced, and includes driving limited to pre-selected routes, whose typical driving cycles have not been defined. In [35], a systematic approach to estimate the energy consumption of BEVs for real driving conditions is developed by applying statistics. Although the results are attractive, the study lacks methodologies to define typical driving cycles of the predefined routes. Consistent with this approach, a simplified analytical function for estimating the energy consumption of a BEV is derived in [36]. The real-world driving cycles used were collected from conventional vehicle on-board tracking systems and include different city and highway driving conditions.

Ref. [37] evaluates the performance and energy consumption of a BEV in the city of Quito based on the measurement of SOC, total distance traveled, and vehicle speed. For this purpose, they used a BYD e6 that circulated six times around a combined route comprising city and highway sections, with a total of distance 55.8 km; they considered the variation of the slope of the road. However, certain inadequacies were detected that could make the results inaccurate, namely, the small number of tests performed, the lack of a TDC definition for the selected route, the SOC measurement performed from the dashboard every 2 min, and the vehicle speed obtained through GPS.

Finally, in [38], the energy efficiency behavior of a BEV in Cuenca is analyzed, considering factors such as orography and traffic conditions on three predefined routes; their TDCs are not defined. In addition, three laboratory driving cycle tests were carried out: FTP-75, NEDC, and WLTP. The data from each sample contain 154 variables of interest, obtained through OBD2, which then underwent a correlation analysis to identify those that affected the BEV's energy performance in the six operating scenarios.

Table 1 presents a summary of the literature presented on studies aimed at estimating the energy consumption in passenger cars BEVs, discerning the methodology used, the application of standardized driving cycles or real-world driving conditions, the definition of the typical driving cycle (TDC) and the consideration of the slope profile. The present proposal is included in Table 1 to observe the differences with respect to the literature cited in the previous paragraphs.

Table 1. Literature on estimating energy consumption in tourism EVs.

Ref.	Methods/Software	Standardized Driving Cycles	Real-World Driving Conditions	Definition of TDC	Considers Slope Profile
[27]	Microtrips, simulation in Advisor software		•	•	
[28]	Digital twins, GT-Suite software	•			
[1]	Statistical regressions, R software and Python		•		
[29]	Longitudinal dynamic model		•		
[30]	Integral propulsion system model and longitudinal dynamics, MATLAB/Simulink	•			
[31]	Power-based EV energy consumption model (CPEM). Numerical model based on the	•			
[32]	vehicle's technical and operational parameters	•			
[33]	Artificial neural networks		•		•
[34]	Analytical model for estimating instantaneous power and energy, Microsoft Excel.	•	•		•

Table 1. Cont.

Ref.	Methods/Software	Standardized Driving Cycles	Real-World Driving Conditions	Definition of TDC	Considers Slope Profile
[35]	Polynomial model, SPSS software.		•		•
[36]	Statistical method based on physics.		•	• Gasoline-powered vehicles	•
[37]	SoC measurement from dashboard, total travel distance and vehicle speed via GPS.		•		•
[38]	Statistical correlation	•	•		•
This article	Model-driven approach for estimating instantaneous power and energy; deterministic method of Minimum weighted differences of the characteristic parameters (MWD-CP), MATLAB/Simulink.		•	• Cab racing only	•

3. Contribution and Novelty of the Study

Unlike the research mentioned in the previous section, it is worth noting the contributions of the present work to expand the field of knowledge about electric vehicles in real driving conditions in an Andean city, defining the TDC. Specifically, no research has been conducted in the region with the level of detail and relevant methodological aspects proposed in this article, which seeks to serve as an input for the promotion of electric vehicles in Latin America and worldwide. Concomitant to this, the application of the weighted minimum difference methodology to estimate the TDC, whose characteristic parameters are the energies of the various forces that oppose the vehicle's motion, is somewhat novel, as demonstrated in [39]. Also, it is relevant that the effects of the road gradient are considered for the purpose of weighing the energy consumption and that the slope smoothing has been performed in a different and methodical way, starting from the correction of the instantaneous altitude data of the vehicle with the EU 646 regulation, shown in [40]. It is worth mentioning that, in the dynamic model of the electric cab, a variable mass that depends on the passengers makes the results more conclusive. Another contribution is the experimental weighing of the efficiency of the electric motor using its efficiency map and the variables of the percentage of accelerator pedal load and the engine speed for each monitored day. And, finally, the BEV used in this research provides its services as a means of public transportation in the cab modality; this is something that has not been studied.

4. Materials and Methods

4.1. Experimental Unit and Data Acquisition Method

The electric cab used in the research is the KIA SOUL EV (KIA, Seoul, Republic of Korea), equipped with an AC permanent magnet synchronous motor, with a maximum torque and power of 285 Nm and 81.4 kW, respectively. It also has a lithium-ion polymer battery bank, with a storage capacity of 27 kWh. On the other hand, the experimental scenario comprises the free travel of the electric cab in the urban area of the city of Loja, whose average altitude of 2060 m above sea level was taken into account in the calculation of air density. Since the vehicle circulates at a higher altitude, the air density will have lower values and, consequently, there will be lower air resistance as well. Thus, an air density of 0.88 kg/m³ was considered.

The unit was monitored for one month, during daily working days, acquiring in real time the speed, geographical variables, accelerator pedal position, current, and battery voltage, through the OBDII port of the KIA SOUL EV, using a data logger device, model

OBDLink MX+, which includes GPS, at a sampling rate of 1 Hz. The reading and storage of variables were performed with a program code developed in Labview (version 2020), used in previous investigations [41,42]. In addition, the initial and final time of each ride with passengers was recorded manually, and the number of passengers was also counted. This allowed us to obtain a variable mass of the unit in service. That is, when the cab circulates without passengers, the value of the mass of the cab considers the empty weight of the vehicle, which was 1492 kg, plus the weight of the driver, which was 70 kg. When the cab circulated with passengers, the mass of the unit varied according to the number of passengers. NTE INEN 1323:2009, as detailed in [43], stipulates that the mass of an occupant can be estimated at 70 kg. Figure 6 shows the satellite map of the electric cab route on day 3, with a total of 49,775 monitored data points. EU Regulation 646 introduces provisions regarding pollutant emissions from passenger cars and light commercial vehicles and their assessment. In particular, it details testing and type-approval requirements. In addition, it presents an appendix with the calculation procedures for verifying the overall vehicle path dynamics. This regulation is important for this research in order to establish the slope profile to be used in the vehicle dynamic model.

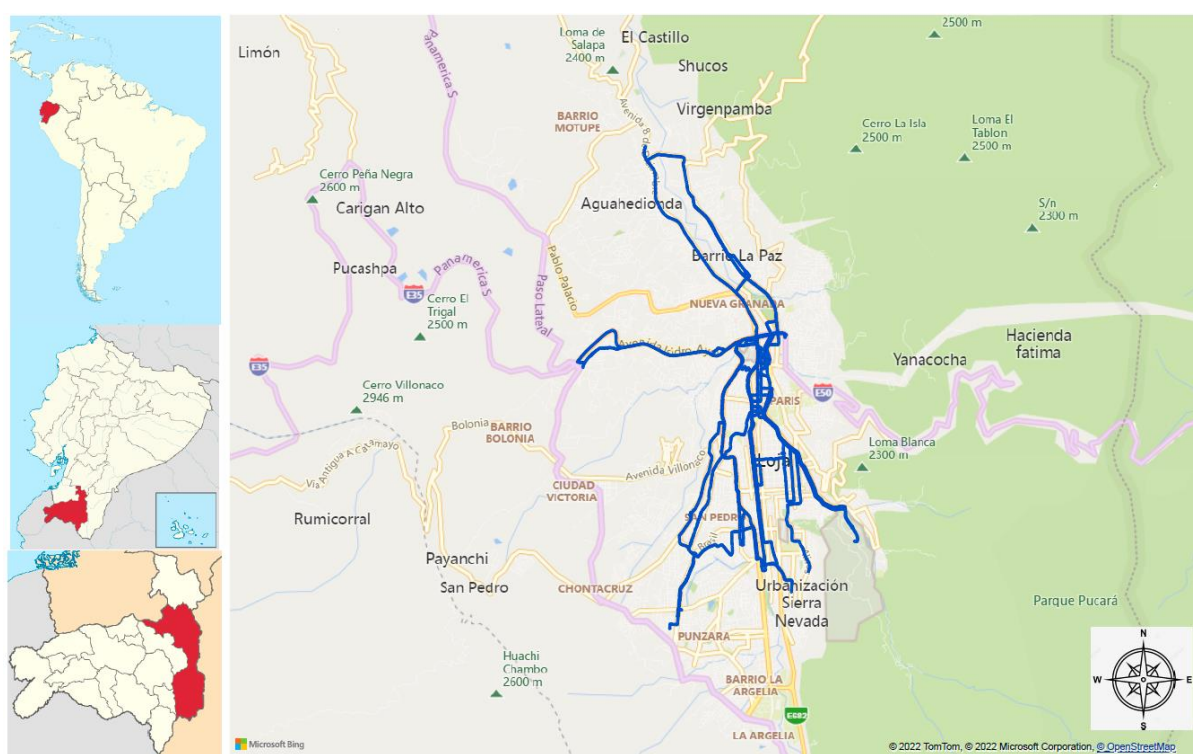


Figure 6. Satellite map of the EV path on day 3.

The EU 646 regulation considers four sequential processes of altitude smoothing and two of slope smoothing, where the BEV geographic data were measured with the GPS OBDLink and the BEV geographic data according to the topographic map, which in this case is the digital terrain model provided by the online application GPS Visualizer [44], where the monitored values of latitude and longitude of the vehicle are introduced. It should be emphasized that this application is free and creates maps and profiles from geographic data. The smoothing starts by taking as a starting point the geographical variables of latitude, longitude, and instantaneous altitude of the vehicle. Thus, Figure 7 shows the final altitude smoothing for run 1 on day 24. Meanwhile, Figure 8 shows the final slope smoothing when compared with the slope profile obtained with GPS Visualizer.

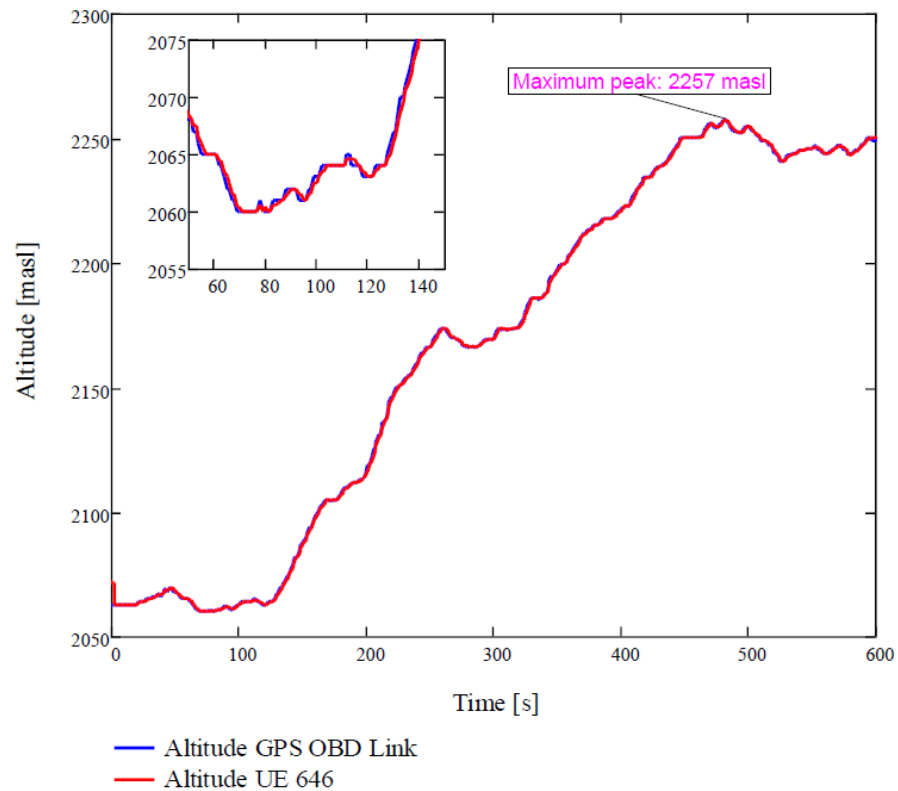


Figure 7. EV altitude profile for run 1 on day 24.

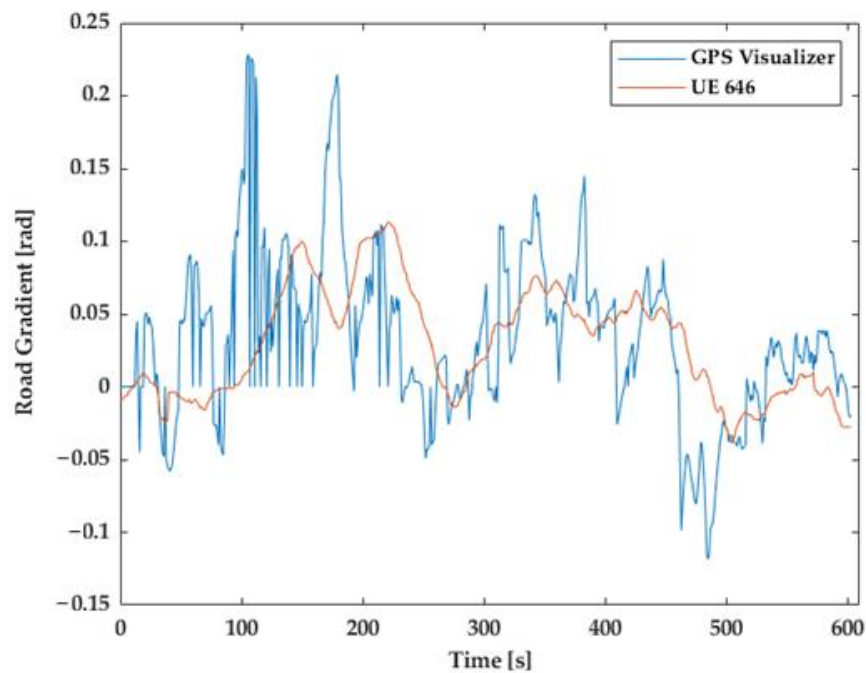


Figure 8. Road gradient for run 1 on day 24.

On the other hand, to obtain the torque curve and the engine efficiency map, a SuperFlow chassis dynamometer (Superflow, Sussex, WI, USA), model AutoDyn 30, with a single set of rollers with a diameter of 76.2 cm, where the BEV is anchored, as shown in Figure 9, was used.



Figure 9. BEV located on the chassis dynamometer.

Figure 10 shows the resulting torque curve and compares it with that given by the manufacturer [45], showing its similarity. The maximum experimental torque reached is 281 Nm.

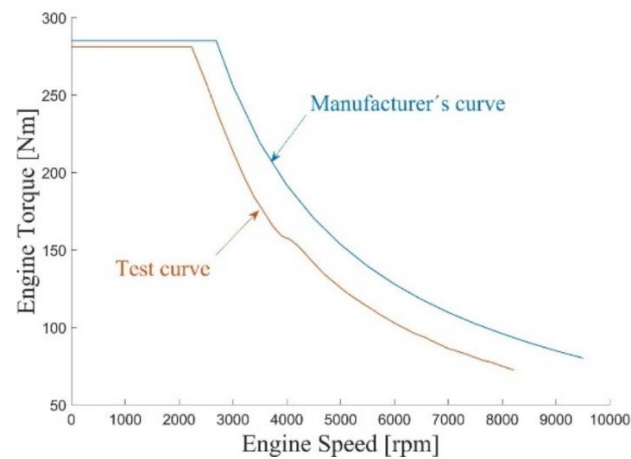


Figure 10. EV motor torque curve.

To obtain the electric motor efficiency map, 20 random tests were performed, where different linear speed and throttle load percentage scenarios were applied. Figure 11 shows the BEV electric motor efficiency map.

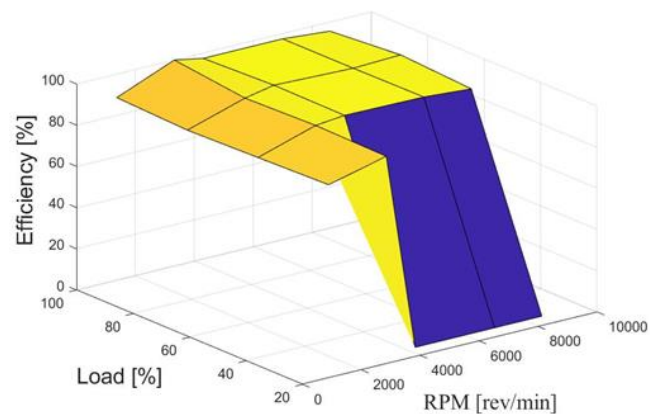


Figure 11. Electric motor efficiency map.

4.2. Model

4.2.1. Longitudinal Dynamics of the Vehicle

According to Newton's law of motion, the acceleration of the vehicle satisfies the following differential equation [46,47].

$$m \cdot \frac{dv(t)}{dt} = F_x(t) - F_r(t) \quad (1)$$

where F_x is the tractive force that must be provided by the motor to the wheels for the vehicle to move [48]. F_r is the sum of the drag forces and m is the total mass of the vehicle, including the rotating parts; F_r comprises the rolling resistance R_x , the aerodynamic drag force F_d , and the gravitational force related to the inclination of the vehicle R_g . Under this context, and by clearing F_x , Equation (1), which represents the equation of the longitudinal motion of the vehicle, can be rewritten as shown in Equation (2) [49]. It should be noted that $m \cdot \frac{dv}{dt}$ was substituted for the inertia force R_i .

$$F_x = F_d + R_x + R_g + R_i \quad (2)$$

Equations (3)–(5) show the equivalences of the various resistance forces [35].

$$R_x = f_r mg \cos \theta \quad (3)$$

$$R_g = mg \sin \theta \quad (4)$$

$$F_d = \frac{1}{2} C_d A \rho_a (V)^2 \quad (5)$$

where V is the vehicle speed and θ is the slope of the road in radians. The terminology used in the previous equations, as well as the associated values, are detailed in Table 2. Figure 12 represents the longitudinal diagram of the vehicle showing the forces required and the force generated at the wheel.

Table 2. Variables of the longitudinal dynamics of the BEV.

Variable	Description	Value	Unit
f_r	Rolling resistance coefficient	0.017 [41]	–
g	Gravity	9.81	m/s ² .
C_d	Aerodynamic coefficient	0.35 [41]	–
A	Front area of the vehicle	2.3 [41]	m ²
ρ_a	Air density	0.88	kg/m ³ ;

4.2.2. Torque, Power, and Wheel Energy

The wheel torque was obtained with Equation (6) [50], where r_d is the dynamic radius with a value of 0.31 m, obtained by calculation based on the wheel designation.

$$\tau_x = F_x \cdot r_d \quad (6)$$

The power required for a vehicle traveling at a given speed can be estimated using the following equation [34]:

$$p_x = F_x \cdot V = \left(ma + \frac{1}{2} C_d A \rho_a V^2 + mg \sin \theta + mg f_r \cos \theta \right) V \quad (7)$$

On the other hand, the total energy consumption, understood as the total electricity use for a trip, was calculated by integrating the power during the travel time T , as shown in the equation below [39]:

$$e_x = \int_0^T p_x(t) dt \quad (8)$$

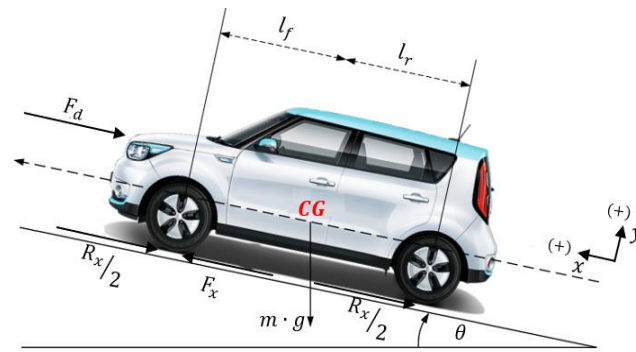


Figure 12. Force diagram for the longitudinal dynamics of the vehicle.

$e_x(+)$ is considered, since this is what is needed to provide traction and move the vehicle [51]. The negative energy is channeled through the BEV regeneration system. The positive energy of the different forces that oppose the movement of the vehicle will be equal to the energy demand or consumption.

4.2.3. Power and Discharge Energy

The calculation of the angular velocity of the motor commences with Equation (9), where N_{td} is the total gear ratio, set at 8.206 according to the BEV manufacturer's data.

$$w_e = \frac{V \cdot N_{td} \cdot 30}{r_d \cdot \pi} \quad (9)$$

Then, using Equation (10), the required torque to the electric motor was determined.

$$T_m = \frac{(F_x + m_e \cdot a) \cdot r_d}{N_{td} \cdot \eta_{td}} \quad (10)$$

where η_{td} is the transmission efficiency, with a value of 0.93 [40,41], a is the acceleration of the vehicle, and m_e is the equivalent mass. Together, these last two make up the rotational inertia losses.

The discharge power of the motor was calculated with Equation (11), where η_m is the motor efficiency, with an average of 0.88, obtained experimentally using the motor efficiency map and the measured variables, i.e., the position of the accelerator pedal and the angular velocity of the electric motor, for each monitored day.

$$P_D = \frac{T_m \cdot w_e}{\eta_m} \quad (11)$$

Finally, the discharge energy was calculated using Equation (12):

$$E_D = \int_0^T P_D dt \quad (12)$$

4.2.4. Energy Regeneration

The regenerative braking power, or charging power, of the BEV can be defined by Equation (13) [52,53].

$$P_c = k \eta_{td} \eta_m F_x V + P_{accessorios} \quad (13)$$

where k ($0 < k < 1$) is the regenerative braking factor, which indicates the percentage of the total braking energy that can be recovered by the motor. The regenerative braking factor is defined according to the conditions given in (14).

In addition, Equation (13) considers the effects of accessories on the BEV electrical power consumption. For the present study, the accessory power is close to 800 W, considering certain consumers referred to in [30] that are applied in the electric cab.

$$k = \left\{ \begin{array}{ll} 0.5 \frac{V_x}{5} & V_x < \frac{5m}{s} \\ 0.5 + 0.3 \frac{V_x - 5}{20} & V_x \geq 5m/s \end{array} \right\} \quad (14)$$

Figure 13 shows a global scheme of the model developed MATLAB/Simulink, based on the equations detailed in this section (Appendix A).

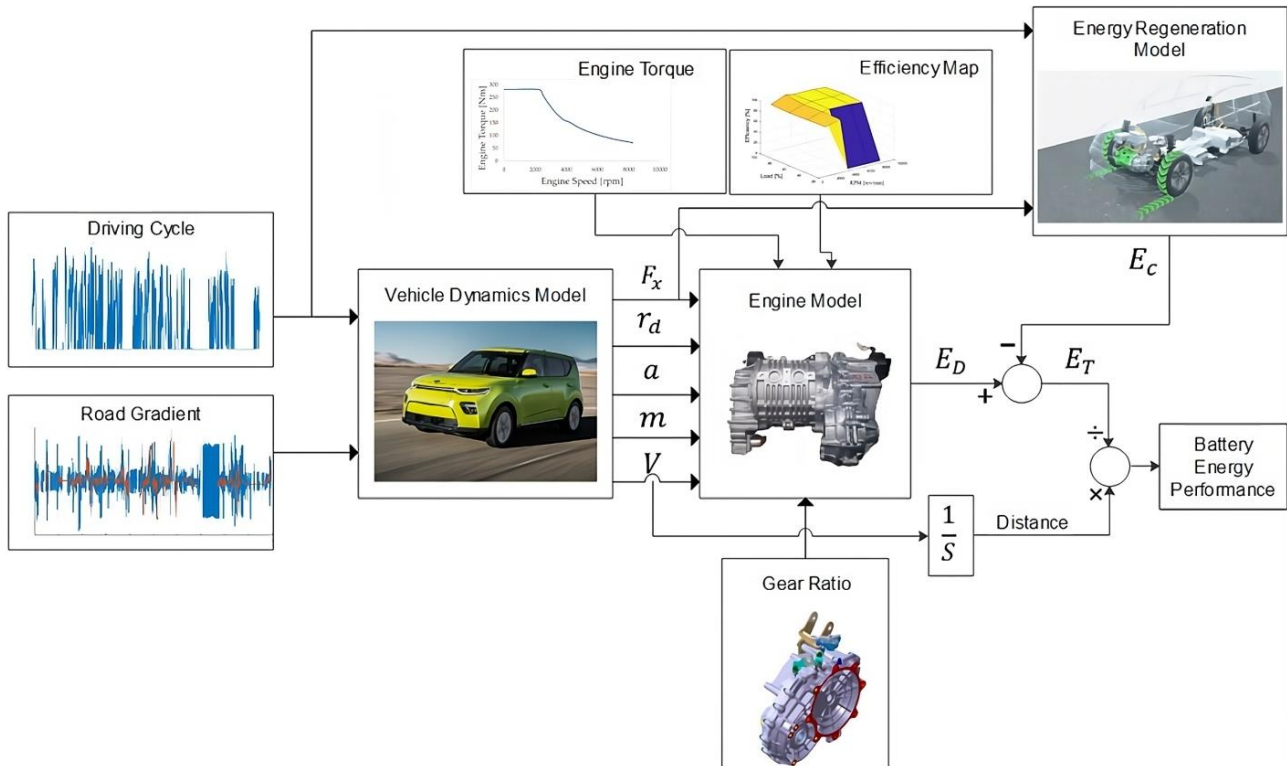


Figure 13. Simulation scheme for EV energy yield estimation.

4.3. Methodology for Defining the TDC

The minimum weighted differences of characteristic parameters (MWD-CPs), a methodology developed by [54], was used to obtain the TDC. The methodology consists of three phases: route selection, driving cycle sampling, and representative cycle selection. The first two phases were already addressed in previous sections of this article. However, it is emphasized that the definition of the TDC focuses specifically on the runs made by the electric cab during the month. That is, it excludes from this analysis the periods when the cab circulates without passengers. Regarding the last phase, the objective is to choose among all the sampled runs the one that represents them, expressing each run in terms of the characteristic parameters or performance values.

P_{ij} was defined as the value of the parameter i obtained for cycle j . First, the arithmetic mean of each parameter was calculated and \bar{P}_i was calculated for all the cycles sampled. The second step consisted of comparing each characteristic parameter with respect to the mean value of the same parameter for all the cycles sampled, $|P_{ij} - \bar{P}_i|$, and then summing the differences obtained for each parameter. However, some parameters are more relevant than others. Therefore, the sum of the differences should be weighted according to the relevance of each parameter in determining, for example, the energy demand, as in [39], where the proposed characterization parameters are the energies demanded by the

types of loads, and their weight will be the percentage of their contribution to the total energy demand.

Finally, as described in Equation (15), the cycle, or run, with the smallest sum of weighted differences is selected as being representative of all cycles in the sample and, therefore, as the TDC.

$$C = \text{Arg} \left\{ \left(\min_j \sum w_i |P_{ij} - \bar{P}_i| \right) \right\} \quad (15)$$

5. Results and Discussion

5.1. General Performance of the Electric Cab in Its Working Day

Regarding the measured linear speed of the electric cab, as shown in Figure 14, an average of 12.95 ± 1.3 km/h per day was obtained. This considers a Student's t distribution and establishes a 95% confidence interval (CI). The highest speed records are reached from 3 to 5 am due to the low influx of vehicles and because the traffic light system remains inactive at those hours. The opposite occurs from 12 am to 1 pm, where traffic is considerable because it is rush hour and the speed drops to an average of 9.39 km/h.

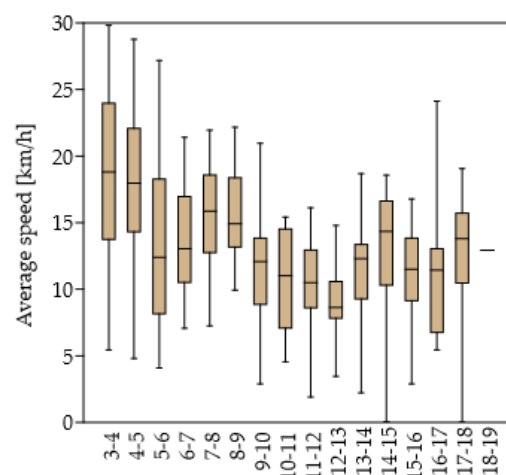


Figure 14. Average BEV velocities by time of day.

On the other hand, the measured battery energy efficiency per hour of the day is shown in Figure 15. The electric cab travels an average of 153 km per day and has an average battery performance of 8.49 ± 1.4 km/kWh, showing congruence with the results of [55] for city driving, with mild weather, and without the use of air conditioning. A higher energy efficiency, that is, 13.41 km/kWh, is highlighted in the 3 to 4 am interval, justified by low traffic conditions, as it occurs with the speed analysis. On the other hand, the lowest energy efficiency, with 3.80 km/kWh, is found between 6 and 7 pm, as this is the hour with the highest traffic congestion.

Regarding traction energy $e_x(+)$, a daily average of $54 \pm 2.4\%$ was obtained when the cab circulated with passengers. During the 24 days of the study, a total of 895 passengers were transported, equivalent to an average of 37.29 passengers per day. That is, almost half of the vehicle's route was driven without passengers, as shown in Figure 16. These data are interesting and could be used by the cab driver to adopt possible strategies to optimize their working day.

Likewise, a daily average of real battery regenerated energy of $31.2 \pm 1.5\%$ was obtained. Figure 17 shows the measured battery regeneration energy for day 3 of the trip, with a duration of 49,775 s and a distance traveled of 165 km. This gives a total demanded battery energy of 29.78 kWh, a total regeneration energy of 8.52 kWh, and as a difference in these two, a net battery energy of 21.26 kWh. When battery energy is demanded, the blue curve rises, and so does the red curve; the green curve remains constant. On the contrary,

when an energy regeneration phenomenon occurs, the green curve rises, while the red curve falls; the blue curve remains constant.

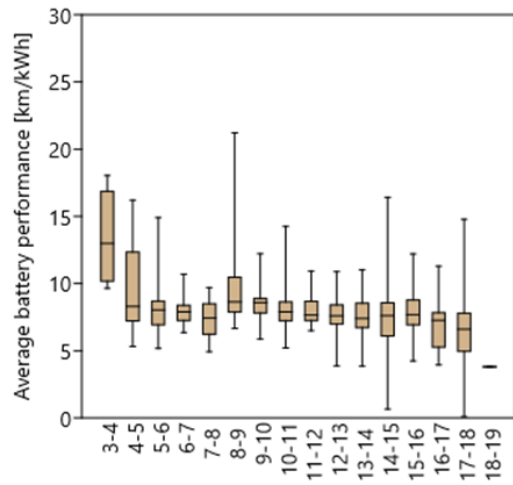


Figure 15. Average BEV energy performance by hours of the day.

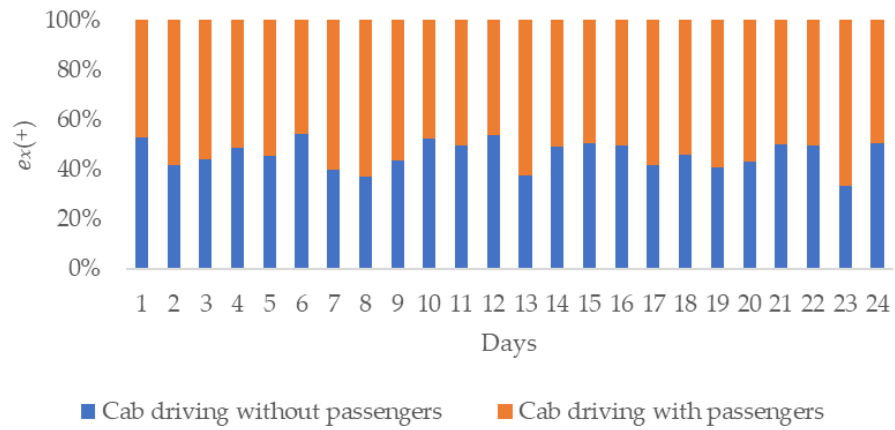


Figure 16. Disaggregation of positive wheel energy by travel condition for the 24 days monitored.

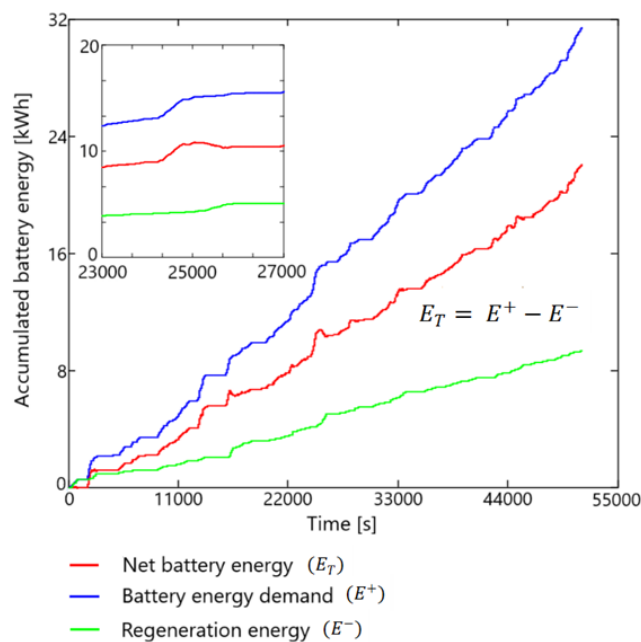


Figure 17. Measured battery energy in the BEV run of day 3.

5.2. Definition of the TDC of the Electric Cab in a Running Condition

The histogram in Figure 18 represents the frequency distributions of the runs classified by time of day. The electric cab made 660 runs in the entire month, ranging from 3 am to 7 pm. The distribution of the data exhibits a considerable predominance of runs in the morning hours, suggesting higher labor productivity. The first quartile (Q1) indicates that 25% of the runs occur until 8 am. The second quartile, Q2, which is the median value, indicates that half of the runs occur until 10 am. Q3 states that three quarters of the runs take place until 1 pm. Per month, the cab performed the most runs, 75 in total, in the 8–9 am time slot, and only one run in the 6–7 pm time slot.

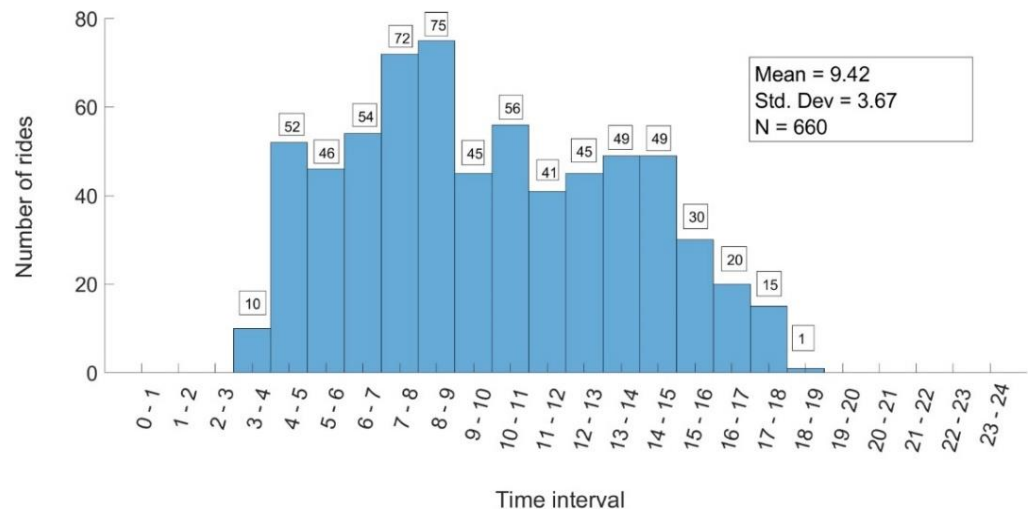


Figure 18. Histogram of rides per hour a day.

Table 3 summarizes the results derived from the deterministic MWD-CP methodology. The TDC corresponds to run 5 of day 11, with a sum of weighted differences of 0.25; this is the lowest among all 660 runs. In addition, it presents a traction energy efficiency of 5.96 km/kWh. Of the characteristic parameters, the percentage of energy demanded by inertia stands out in first place, at 49.48%, and in last place is the percentage of energy demanded by aerodynamic drag, at 3.48%.

Table 3. $e_x(+)$ per run: TDC.

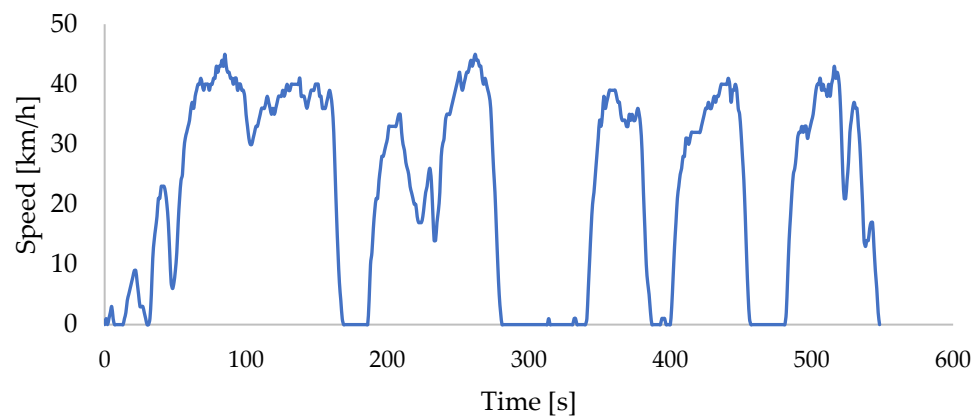
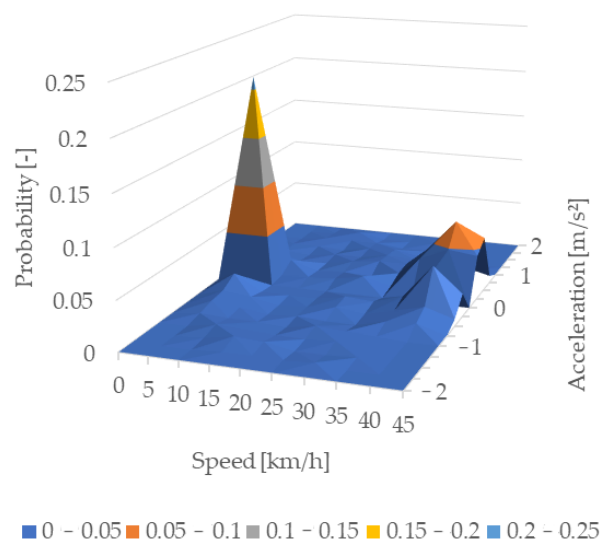
Day	Ride	% $EF_d(+)$	% $ER_x(+)$	% $ER_g(+)$	% $ER_i(+)$	Σ
11	5	3.48	27.82	19.22	49.48	0.25

In addition, Table 4 shows the parameters related to the TDC. Among them, it highlights a run duration of 9 min and 8 s, where 3.4 km were traveled, with a passenger on board. The ratio of the acceleration and deceleration state of the obtained TDC can be associated by traffic congestion conditions in the urban area where the electric cab circulates [56].

The TDC obtained for the electric cab by the proposed method is shown in Figure 19. Figure 20 depicts the speed–acceleration probability distribution (SAPD) of the established real-world driving cycle. From this, it can be seen that the velocity probability is highest for the range of 0 to 10 km/h and the acceleration is mainly distributed between -0.5 to 0.5 m/s^2 . These results indicate that the electric cab starts and stops several times, accelerations and decelerations are frequent, and the velocity is low, in agreement with the findings of [57]. These driving conditions are typical of a vehicle circulating in an urban area, where traffic is heavy and there are traffic lights.

Table 4. TDC parameters.

Designation	Value	Unit
Duration	548	[s]
Distance	3.4	[km]
Average speed	22.32	[km/h]
Maximum speed	45	[km/h]
Proportion of idle time	22.40	[%]
Proportion of cruising	16.58	[%]
Proportion of time accelerating	35.88	[%]
Proportion of time decelerating	25.14	[%]

**Figure 19.** TDC of the electric cab per run.**Figure 20.** Velocity-acceleration probability distribution (SAPD) of the TDC.

Additionally, Table 5 shows the results for the critical driving cycle, i.e., the one with the highest consumption among all the runs. It corresponds to run 2 of day 5, with a sum of weighted differences of 23.13 and a traction energy efficiency of 3.14 km/kWh. The governing characteristic parameter is the energy demanded by inertia, at 54.63%, followed by the energy demanded by the slope, at 23.44%.

Table 5. $e_x(+)$ per run: critical driving cycle.

Day	Ride	% $EF_d(+)$	% $ER_x(+)$	% $ER_g(+)$	% $ER_i(+)$	Σ
5	2	2.92	19	23.44	54.63	23.13

In addition, the SAPD diagram in Figure 21 for the critical cycle shows that the velocity probability is highest for the range of 35 to 45 km/h and acceleration predominates between -0.75 and 0.75 m/s². These values indicate, unlike the TDC, that the driving incorporates a wider range of accelerations, which are evident in the resulting surface.

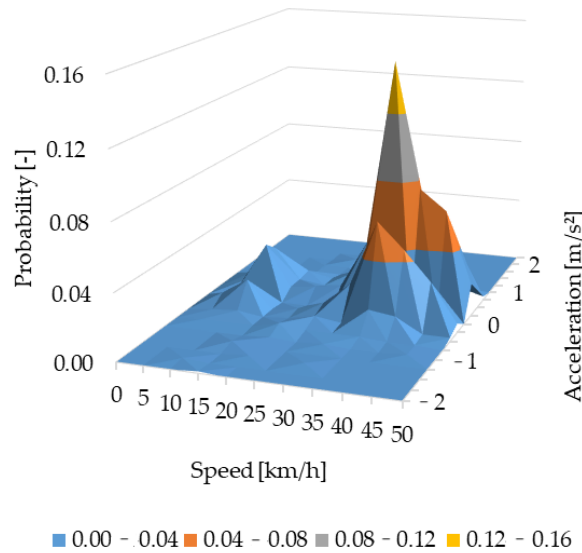


Figure 21. SAPD diagram of the critical driving cycle.

5.3. Validation of the BEV Energy Efficiency Model

In this section, the daily energy yield obtained through the model is validated with respect to the measured values. In the first instance, and considering the size of the samples, the Shapiro–Wilk test is applied to contrast the normality of the data set using Past statistical software (version 4); a significance level of 0.05 is proposed. Figure 22 shows the results obtained. According to the orange box, since the p -value is greater than the significance level for both samples, the null hypothesis is not rejected and it is concluded that the data obey a normal distribution.

	Measurement	Estimation
N	24	24
Shapiro-Wilk W	0.9401	0.9448
p(normal)	0.1636	0.2081
Anderson-Darling A	0.4446	0.3466
p(normal)	0.2608	0.4516
p(Monte Carlo)	0.2644	0.4529
Lilliefors L	0.1435	0.09146
p(normal)	0.2201	0.8695
p(Monte Carlo)	0.2102	0.8635
Jarque-Bera JB	1.276	1.257
p(normal)	0.5283	0.5333
p(Monte Carlo)	0.3271	0.3241

Figure 22. Results of the Shapiro-Wilk test.

Once the normality of the data set was corroborated, Pearson’s parametric correlation test was applied to evaluate the linear dependence between the quantitative variables under study. A Pearson’s correlation coefficient r of 0.93 was obtained, denoting a strong and positive correlation between them, as can be seen in the correlogram in Figure 23.

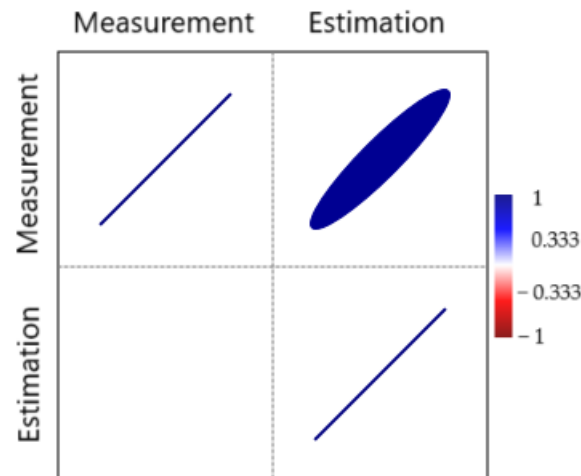


Figure 23. Correlogram of the pair of variables under study.

In addition, to evaluate the prediction accuracy, dependent on the relationship between the variables under study, the coefficient of determination R^2 was calculated. The point spread of the variables with respect to the regression line is shown in Figure 24. An R^2 of 0.86 was obtained, which expresses that the model has a satisfactory predictive capacity for battery performance, surpassing the results achieved by [35], with an R^2 of 0.77.

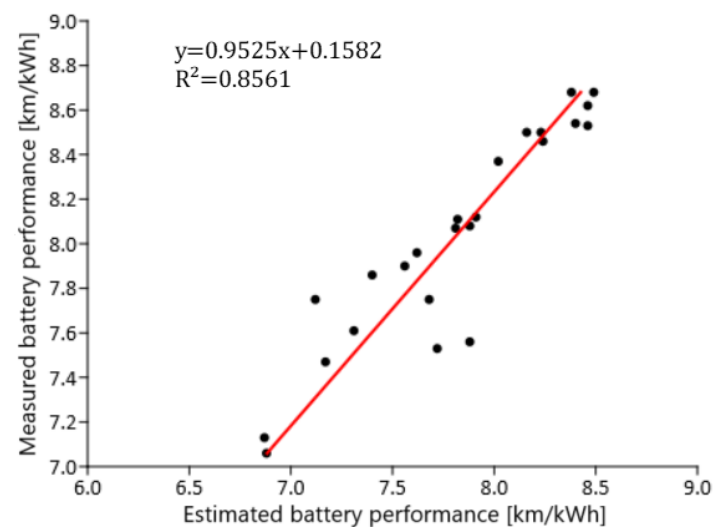


Figure 24. Goodness of fit of the predictive model based on the coefficient of determination.

Finally, the mean absolute percentage error (MAPE) was calculated for the 24-day energy yield values shown in Figure 25.

The MAPE is defined by Equation (16) [34].

$$\text{MAPE} = \frac{1}{n} \sum_{i=1}^n \left| \frac{E_m - E_e}{E_m} \right| \times 100\% \quad (16)$$

where E_m is the measured energy performance, E_e is the estimated energy performance, and n is the number of evaluated data. The MAPE obtained is 3.35%, which shows an adequate fit between the model estimates and measurements. This result is similar to that obtained by [31], where the prediction errors are less than 3%, and it exceeds those obtained by [30–32,34], which had errors of 6, 5.9, 4, and 15.6%, respectively.

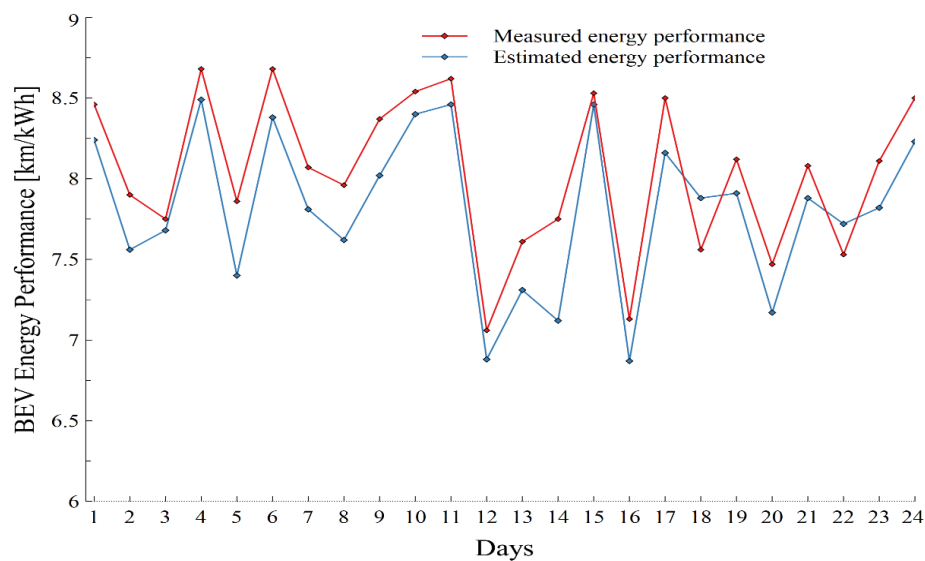


Figure 25. Estimated energy performance of BEV vs. performance measured for 24 days.

6. Conclusions

The purpose of this study was to estimate, through a model-driven approach developed in MATLAB/Simulink, the energy performance of an electric vehicle operating as a cab in the urban area of the city of Loja, Ecuador. From the results obtained, it is concluded that the electric cab traveled an average of 153 km per day and had an average measured battery performance of 8.49 ± 1.4 km/kWh, where the actual energy regenerated from the battery was $31.2 \pm 1.5\%$.

The cab made 660 runs in the course of a month, of which three quarters occurred in the 12–1 pm period, suggesting a higher labor productivity in the morning hours. The TDC of the cab when driving with passengers corresponds to run 5 on day 11, with a sum of weighted differences of 0.25 and a traction energy efficiency of 5.96 km/kWh. The characteristic parameters used were the energies of the various forces opposing the vehicle's movement, with inertia demanding the most energy (49.48%). The TDC had a duration of 9 min and 8 s, during which the electric cab traveled 3.4 km, with a passenger on board. A high proportion of TDC acceleration and deceleration states was shown, with 33.88% and 25.14%, respectively. These values are associated with real-world driving conditions in the urban area of the city where traffic and traffic lights play a predominant role. This also justifies the low speed of the unit, with an average of 22.32 km/h. Through the SAPD diagram, it was identified that the speed probability is higher for the range of 0 to 10 km/h and the acceleration is distributed between -0.5 to 0.5 m/s². In addition, with a daily average of $54 \pm 2.4\%$ of the traction energy, the cab circulated with passengers. This finding clearly suggests that electric cab drivers should adopt possible strategies to optimize their working day.

To validate the energy yield obtained through the proposed model, the predicted results were compared with the 24-day measured values. A Pearson correlation coefficient of 0.93 was obtained, showing a strong and positive correlation between the variables under study. In addition, a determination coefficient of 0.86 was obtained, which shows that the model has a satisfactory predictive capacity for battery performance. In line with these findings, the MAPE of 3.35% suggests a good fit between the model estimates and the measurements under real driving conditions.

Regarding the limitations of the study, it should be noted that the value of the power of the vehicle accessories was generalized based on the available literature. The measurement of the auxiliary loads of the electric vehicle could be a subsequent study in order to improve the results achieved in the proposed model. On the other hand, the rolling resistance coefficient and the aerodynamic coefficient were set at a constant value. However, it would

be interesting in future work to consider their variation at a higher level of detail as a function of vehicle operating conditions. In addition, the monitoring frequency of the vehicle variables was limited to 1 Hz; therefore, it would be essential to evaluate in a future work the energy consumption of the electric vehicle at a higher frequency rate. Furthermore, the present investigation is limited to an electric vehicle used for passenger transport, so in future work it is planned to evaluate the energy consumption of electric vehicles used for freight transport.

Finally, the methodology proposed with the described model can be generalized and used with other electric vehicles. However, it is imperative to acknowledge that the outcomes regarding energy performance will inherently vary based on individual vehicle specifications, prevailing driving conditions, the vehicle's intended use, and the external environmental factors pertinent to the study location.

Author Contributions: Conceptualization, J.C.-C., D.C.-M. and E.L.P.; methodology, J.C.-C. and D.C.-M.; validation, D.C.-M. and E.L.P.; formal analysis, J.C.-C. and D.C.-M.; research, J.C.-C.; resources, J.C.-C.; data curation, J.C.-C.; writing—original draft preparation, J.C.-C.; writing—review and editing, J.C.-C., D.C.-M. and E.L.P.; supervision, D.C.-M. All authors have read and agreed to the published version of the manuscript.

Funding: This research received no external funding.

Data Availability Statement: The data presented in this study are available on request from the corresponding author.

Conflicts of Interest: The authors declare no conflicts of interest.

Appendix A

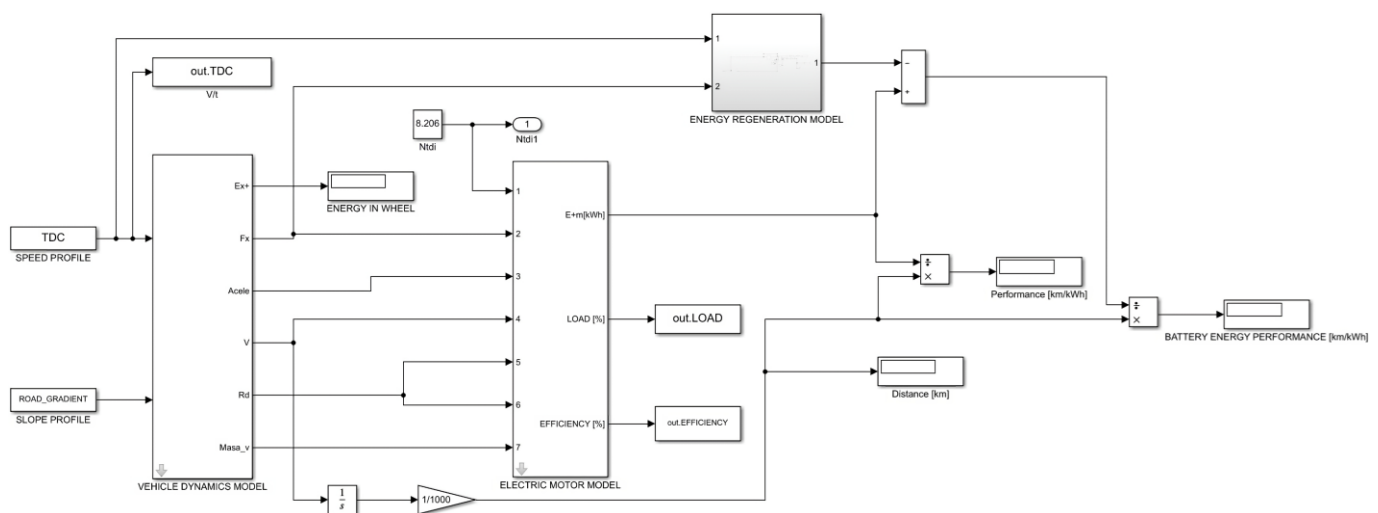


Figure A1. Electric vehicle energy consumption model in MATLAB/Simulink.

References

- Jonas, T.; Hunter, C.; Macht, G. Quantifying the impact of traffic on the energy consumption of electric vehicles. *World Electr. Veh. J.* **2022**, *13*, 15. [CrossRef]
- Huber, D.; De Clerck, Q.; De Cauwer, C.; Sapountzoglou, N.; Coosemans, T.; Messagie, M. Vehicle to Grid Impacts on the Total Cost of Ownership for Electric Vehicle Drivers. *World Electr. Veh. J.* **2021**, *12*, 236. [CrossRef]
- Omahne, V.; Knez, M.; Obrecht, M. Social Aspects of Electric Vehicles Research—Trends and Relations to Sustainable Development Goals. *World Electr. Veh. J.* **2021**, *12*, 15. [CrossRef]
- Gustafsson, M.; Svensson, N.; Eklund, M.; Fredriksson, B. Well-to-wheel climate performance of gas and electric vehicles in Europe. *Transp. Res. Part D* **2021**, *97*, 102911. [CrossRef]
- Daina, N.; Sivakumar, A.; Polak, J.W. Modelling electric vehicles use: A survey on the methods. *Renew. Sustain. Energy Rev.* **2017**, *68*, 447–460. [CrossRef]

6. Ajanovic, A.; Haas, R. Dissemination of electric vehicles in urban areas: Major factors for success. *Energy* **2016**, *115*, 1451–1458. [CrossRef]
7. IEA. Global EV Outlook 2021. Available online: <https://www.iea.org/reports/global-ev-outlook-2021> (accessed on 16 September 2023).
8. Guerrero, J.D.; Bhattarai, B.; Shrestha, R.; Acker, T.L.; Castro, R. Integrating electric vehicles into power system operation production cost models. *World Electr. Veh. J.* **2021**, *12*, 263. [CrossRef]
9. Ye, F.; Kang, W.; Li, L.; Wang, Z. Why do consumers choose to buy electric vehicles? A paired data analysis of purchase intention configurations. *Transp. Res. Part A* **2021**, *47*, 14–27. [CrossRef]
10. IEA. Global EV Outlook 2023. Available online: <https://iea.blob.core.windows.net/assets/dacf14d2-eabc-498a-8263-9f97fd5dc327/GEVO2023.pdf> (accessed on 21 October 2024).
11. Capuder, T.; Miloš Sprčić, D.; Zoričić, D.; Pandžić, H. Review of challenges and assessment of electric vehicles integration policy goals: Integrated risk analysis approach. *Int. J. Electr. Power Energy Syst.* **2020**, *119*, 105894. [CrossRef]
12. Febransyah, A. Predicting Purchase Intention towards Battery Electric Vehicles: A Case of Indonesian Market. *World Electr. Veh. J.* **2021**, *12*, 240. [CrossRef]
13. AEADE. Anuario 2023. Available online: https://www.aeade.net/sdm_downloads/anuario-2023/ (accessed on 22 October 2024).
14. Clairand, J.; González, M. What Is the Level of People’s Acceptance for Electric Taxis and Buses? Exploring Citizens’ Perceptions of Transportation Electrification to Pay Additional Fees. *World Electr. Veh. J.* **2022**, *13*, 3. [CrossRef]
15. Jaramillo, W. Taxis eléctricos en la ciudad de Loja-Ecuador. *Espacios* **2019**, *40*, 18.
16. Díaz, J.; Castillo-Calderón, J. Estimación del indicador kilómetro vehículo recorrido (KVR) mediante ecuaciones lineales y sus aplicaciones en consumos energéticos de transporte. *Inf. Tecnológica* **2021**, *32*, 239–254. [CrossRef]
17. Sierra, J.C. Estimating road transport fuel consumption in Ecuador. *Energy Policy* **2016**, *92*, 359–368. [CrossRef]
18. MERNNR. Balance Energético Nacional 2020. Available online: <https://www.ambiente.gov.ec/wp-content/uploads/downloads/2021/09/Balance-Energetico-Nacional-2020-Web.pdf> (accessed on 10 October 2023).
19. Icaza, D.; Borge-Diez, D.; Pulla, S. Analysis and proposal of energy planning and renewable energy plans in South America: Case study of Ecuador. *Renew. Energy* **2022**, *182*, 314–342. [CrossRef]
20. Arévalo, P.; Cano, A.; Benavides, D.; Aguado, J.; Jurado, F. Energy transition in Ecuador, a proposal to improve the growth of renewable energy and storage systems in a developing country. In *Energy Efficiency of Modern Power and Energy Systems*; Elsevier: Amsterdam, The Netherlands, 2024; pp. 19–31. [CrossRef]
21. Icaza, D.; Jurado, F.; Tostado-Véliz, M. Long-term planning for the integration of electric mobility with 100% renewable energy generation under various degrees of decentralization: Case study Cuenca, Ecuador. *Energy Rep.* **2023**, *9*, 4816–4829. [CrossRef]
22. Arévalo, P.; Tostado-Véliz, M.; Montaleza, C.; Jurado, F. Integration of renewable energies and electric vehicles in interconnected energy systems. In *Sustainable Energy Planning in Smart Grids*; Elsevier: Amsterdam, The Netherlands, 2024; pp. 351–359. [CrossRef]
23. Castro, P.; Vidoza, J.; Gallo, W. Analysis and projection of energy consumption in Ecuador: Energy efficiency policies in the transportation sector. *Energy Police* **2019**, *134*, 110948. [CrossRef]
24. IEA. Energy Technology Perspectives 2020. Available online: https://iea.blob.core.windows.net/assets/7f8aed40-89af-4348-be19-c8a67df0b9ea/Energy_Technology_Perspectives_2020_PDF.pdf (accessed on 15 October 2023).
25. Moeletsi, M.E. Socio-Economic Barriers to Adoption of Electric Vehicles in South Africa: Case Study of the Gauteng Province. *World Electr. Veh. J.* **2021**, *12*, 167. [CrossRef]
26. Diario Crónica. A Los Taxis Eléctricos Pueden Cambiarlos a Convencionales Tras Aprobación de Reforma. Available online: <https://cronica.com.ec/2022/07/14/a-los-taxis-electricos-pueden-cambiarlos-a-convencionales-tras-aprobacion-de-reforma/> (accessed on 17 October 2023).
27. Sun, D.; Zheng, Y.; Duan, R. Energy consumption simulation and economic benefit analysis for urban electric commercial-vehicles. *Transp. Res. Part D Transp. Environ.* **2021**, *101*, 103083. [CrossRef]
28. Xie, Y.; Li, Y.; Zhao, Z.; Dong, H.; Wang, S.; Liu, J.; Guan, J.; Duan, X. Microsimulation of electric vehicle energy consumption and driving range. *Appl. Energy* **2020**, *267*, 115081. [CrossRef]
29. Wager, G.; Whale, J.; Braunl, T. Driving electric vehicles at highway speeds: The effect of higher driving speeds on energy consumption and driving range for electric vehicles in Australia. *Renew. Sustain. Energy Rev.* **2016**, *63*, 158–165. [CrossRef]
30. Miri, I.; Fotouhi, A.; Ewin, N. Electric vehicle energy consumption modelling and estimation—A case study. *Int. J. Energy Res.* **2020**, *45*, 501–520. [CrossRef]
31. Fiori, C.; Ahn, K.; Rakha, H.A. Power-based electric vehicle energy consumption model: Model development and validation. *Appl. Energy* **2016**, *168*, 257–268. [CrossRef]
32. Gołębiewski, W.; Lisowski, M. Theoretical analysis of electric vehicle energy consumption according to different driving cycles. *IOP Conf. Ser. Mater. Sci. Eng.* **2018**, *421*, 022010. [CrossRef]
33. Jimenez, F.; Amarillo, J.C.; Naranjo, J.E.; Serradilla, F.; Diaz, A. Energy Consumption Estimation in Electric Vehicles Considering Driving Style. In Proceedings of the IEEE 18th International Conference on Intelligent Transportation Systems, Gran Canaria, Spain, 15–18 September 2015; pp. 101–106. [CrossRef]
34. Wu, X.; Freese, D.; Cabrera, A.; Kitch, W.A. Electric vehicles’ energy consumption measurement and estimation. *Transp. Res. Part D Transp. Environ.* **2015**, *34*, 52–67. [CrossRef]

35. Zhang, R.; Yao, E. Electric vehicles' energy consumption estimation with real driving condition data. *Transp. Res. Part D Transp. Environ.* **2015**, *41*, 177–187. [CrossRef]
36. Yuan, X.; Zhang, C.; Hong, G.; Huang, X.; Li, L. Method for evaluating the real-world driving energy consumptions of electric vehicles. *Energy* **2017**, *141*, 1955–1968. [CrossRef]
37. Diaz, J.; Guillén, J.; Arroyo, D.; Maks, M. Performance Evaluation of an Electric Vehicle in Real Operating Conditions of Quito, Ecuador. In Proceedings of the 4th International Congress of Automotive and Transport Engineering (AMMA), Cluj-Napoca, Romania, 17–19 October 2018; pp. 328–337. [CrossRef]
38. Merchán, J.; Gonzalez, L.; Espinoza, J. Energy Efficiency of an Electric Vehicle in a Latin American Intermediate City. In Proceedings of the 2018 International Conference on Smart Energy Systems and Technologies (SEST), Seville, Spain, 10–12 September 2018; pp. 1–6. [CrossRef]
39. Cordero-Moreno, D.; Davalos, D.; Coello, M.; Rockwood, R. Proposed criteria to determine typical vehicular driving cycles using minimum weighted differences. *WIT Trans. Built Environ.* **2017**, *176*, 329–337.
40. REGLAMENTO (UE) 2016/646. Emisiones Procedentes de Turismos y Vehículos Comerciales Ligeros. Available online: <https://www.boe.es/buscar/doc.php?id=DOUE-L-2016-80714> (accessed on 30 October 2023).
41. Valladolid, J.D.; Patino, D.; Gruosso, G.; Correa-Flórez, C.A.; Vuelvas, J.; Espinoza, F. A novel energy-efficiency optimization approach based on driving patterns styles and experimental tests for electric vehicles. *Electronics* **2021**, *10*, 1199. [CrossRef]
42. Valladolid, J.D.; Albarado, R.; Mallahuari, D.; Patiño, D. Experimental Performance Evaluation of Electric Vehicles (EV) Based on Analysis of Power and Torque Losses. In Proceedings of the 2020 IEEE International Conference on Industrial Technology (ICIT), Buenos Aires, Argentina, 26–28 February 2020; pp. 933–938. [CrossRef]
43. NTE INEN 1323:2009. Vehículos Automotores. Carrocerías de Buses. Requisitos, 2009. Available online: <https://es.scribd.com/document/94426733/Norma-Tecnica-Ecuatoriana-NTE-ENEN-1-323-2009> (accessed on 17 November 2023).
44. GPS Visualizer. Available online: <https://www.gpsvisualizer.com/> (accessed on 25 November 2023).
45. Automobile Catalog. Kia Soul EV Engine Horsepower/Torque Curve. Available online: https://www.automobile-catalog.com/curve/2019/2910245/kia_soul_ev.html (accessed on 29 November 2023).
46. Maamria, D.; Gillet, K.; Colin, G.; Chamailard, Y.; Nouillant, C. Computation of eco-driving cycles for Hybrid Electric Vehicles: Comparative analysis. *Control Eng. Pract.* **2018**, *71*, 44–52. [CrossRef]
47. Nault, E.; Colin, G.; Gillet, K.; Chamailard, Y.; Zerar, M.; Dollinger, N.; Nouillant, C. Towards an Analytical Eco-Driving Cycle Computation for Conventional Cars. *IFAC (Int. Fed. Autom. Control.)* **2019**, *52*, 550–555. [CrossRef]
48. Perrotta, D.; Ribeiro, B.; Rossetti, R.J.; Afonso, J.L. On the potential of regenerative braking of electric buses as a function of their itinerary. *Procedia Soc. Behav. Sci.* **2012**, *54*, 1156–1167. [CrossRef]
49. Dridi, S.; Ben Salem, I.; El Amraoui, L. Dynamic modeling of nonlinear longitudinal automotive system using graphically based. In Proceedings of the 7th International Conference on Sciences of Electronics, Technologies of Information and Telecommunications (SETIT), Hammamet, Tunisia, 18–20 December 2016; pp. 349–354.
50. Sankar, S.S.; Xia, Y.; Carmai, J.; Koetniyom, S. Optimal eco-driving cycles for conventional vehicles using a genetic algorithm. *Energies* **2020**, *13*, 4362. [CrossRef]
51. Gao, Z.; Lin, Z.; LaClair, T.J.; Liu, C.; Li, J.-M.; Birky, A.K.; Ward, J. Battery capacity and recharging needs for electric buses in city transit service. *Energy* **2017**, *122*, 588–600. [CrossRef]
52. Yang, S.C.; Li, M.; Lin, Y.; Tang, T.Q. Electric vehicle's electricity consumption on a road with different slope. *Phys. A Stat. Mech. Its Appl.* **2014**, *402*, 41–48. [CrossRef]
53. Yang, S.; Deng, C.; Tang, T.; Qian, Y. Electric vehicle's energy consumption of car-following models. *Nonlinear Dyn.* **2013**, *71*, 323–329. [CrossRef]
54. Huertas, J.; Díaz, J.; Cordero, D.; Cedillo, K. A new methodology to determine typical driving cycles for the design of vehicles power trains. *Int. J. Interact. Des. Manuf.* **2017**, *12*, 319–326. [CrossRef]
55. EV Database. Kia e-Soul. Available online: <https://ev-database.org/car/1289/Kia-e-Soul-39-kWh> (accessed on 9 December 2023).
56. Zhao, X.; Ye, Y.; Ma, J.; Shi, P.; Chen, H. Construction of electric vehicle driving cycle for studying electric vehicle energy consumption and equivalent emissions. *Environ. Sci. Pollut. Res.* **2020**, *27*, 37395–37409. [CrossRef]
57. Sun, Z.; Wen, Z.; Zhao, X.; Yang, Y.; Li, S. Real-world driving cycles adaptability of electric vehicles. *World Electr. Veh. J.* **2020**, *11*, 19. [CrossRef]

Disclaimer/Publisher's Note: The statements, opinions and data contained in all publications are solely those of the individual author(s) and contributor(s) and not of MDPI and/or the editor(s). MDPI and/or the editor(s) disclaim responsibility for any injury to people or property resulting from any ideas, methods, instructions or products referred to in the content.